

NUMERICAL SIMULATIONS OF TURBULENT REACTIVE FLOWS USING A HYBRID LES / PDF METHODOLOGY

João Marcelo Vedovoto

School of Mechanical Engineering
Federal University of Uberlândia
Uberlândia-MG, 38400-902 Brazil
jmvedovoto@mecanica.ufu.br

Aristeu da Silveira Neto

School of Mechanical Engineering
Federal University of Uberlândia
Uberlândia-MG, 38400-902 Brazil
aristeus@mecanica.ufu.br

Luis Fernando Figueira da Silva

Department of Mechanical Engineering
Pontifícia Universidade Católica do Rio de Janeiro
Rio de Janeiro-RJ, 22453-900 Brazil
luisfer@esp.puc-rio.br

Arnaud Mura

Institut Pprime, UPR3346 CNRS
ENSMA and University of Poitiers
BP40109 - 86961, Poitiers, France
arnaud.mura@isae-ensma.fr

ABSTRACT

Time-resolved numerical simulations of fluid flows, such as Large Eddy Simulations (LES), have the capability of simulating the unsteady dynamic of large scale energetic structures. However, they are known to be intrinsically sensitive to inflow conditions the modelling of which may become a crucial ingredient of the computational model. The present work reports LES of both reactive and non reactive turbulent channel flows of methane/air mixtures. The flow configuration and associated conditions correspond to those associated with a reference experimental database that has been obtained at the french aerospace Laboratory of Onera. The focus of our study is placed on the influence of synthetic inlet turbulence in this experimental configuration, and the principal aim is to investigate the sensitivity of the flow dynamics and mixing to inflow conditions. This sensitivity is illustrated for four distinct turbulent inflows obtained from *white noise*, *digital filters*, *the random flow generator (RFG)*, and *synthetic eddy model (SEM)*. Finally the results obtained for reactive flow conditions clearly emphasize the influence of the retained model on the chemical reaction rate statistics. This highlights confirms how relevant are the developments devoted to synthetic turbulence for the computational investigation of turbulent combustion.

1 Introduction

It is well known that a subject of great importance for fluid flow numerical simulations is the prescription of correct and realistic boundary conditions. For outflow conditions, it appears that the use of a buffer zone (Bodony, 2006) or an advective boundary condition (Orlanski, 1976), or even a combination of both, may adequately describe several flow conditions of practical interest. The specification of inflow boundary conditions may also raise several issues. For steady Reynolds Averaged Navier Stokes (RANS) simulations, simple analytical or experimental profiles are retained for mean velocity components and turbulent charac-

teristics. For LES or Direct Numerical Simulations (DNS), however, the inflow data should consist of an unsteady fluctuating velocity signal representative of the turbulent velocity field at the inlet.

There are several ways to remedy this situation, and the existing methods belong to two principal categories: (i) *recycling methods*, in which some sort of turbulent flow is pre-computed, prior to the main calculation, and subsequently introduced at the domain inlet, and (ii) *synthetic turbulence methods*, in which some form of random fluctuation is generated, modulated according to experimental data, and combined with mean inflow. Other appealing strategies have been introduced in the literature, some of them are based on Fourier techniques, and others rely on the Proper Orthogonal Decomposition (POD) introduced by Lumley (1967), see for instance Druault *et al.* (2004).

The present manuscript is organized as follows: first a brief description of recycling methods is provided. Further, synthetic turbulence generators are presented, and the four methods retained in the present work are detailed: (i) the *white noise*, (ii) the method proposed by Klein *et al.* (2003), (iii) the *Random Flow Generator - RFG* introduced by Smirnov *et al.* (2001) and (iv) the *Synthetic Eddy Method - SEM* of Jarrin *et al.* (2009). The synthetic turbulence generators have been implemented in a low Mach number Navier-Stokes solver, the main features of which are presented, including a brief description of both mathematical and numerical aspects. Finally, the paper ends with the application of the above-mentioned synthetic turbulence generators to the numerical simulation of high speed non-reactive and reactive turbulent mixing layers, which were experimentally studied by P. & A. (1977), see also Magre *et al.* (1988).

2 Literature review

The specification of realistic turbulent inflow boundary conditions remains a challenging issue for both LES and DNS. A review of some of the existent methods that deal with such turbulent inlet conditions is provided below.

2.1 Recycling methods

The most accurate method to specify turbulent fluctuations for either LES or DNS would be to run a suitable precursor simulation with the purpose of providing the main simulation with accurate boundary conditions. However, such a procedure has been used only when the turbulence at the inlet can be regarded as a fully developed or a spatially developing boundary layer and in the absence of feedback mechanisms. In these cases periodic boundary conditions in the mean flow direction can be applied to the precursor simulation. In general, the simulation of the precursor flow is initialized with a mean velocity profile perturbed with a few unstable Fourier modes. Instantaneous velocity fluctuations in a plane positioned at a fixed streamwise location are extracted from the precursor simulation and prescribed at the inlet of the main simulation at each time step.

In practice, periodic boundary conditions can only be used to generate inflow conditions for homogeneous flows in the streamwise direction, which restricts their applications to simple fully developed flows. In the present work, we focused our developments searching for a general approach for generating inlet turbulent conditions, hence the resort to synthetic turbulence generators.

2.2 Synthetic turbulence generators

Methods that do not rely on a precursor simulation, or re-scaling of a database obtained from a precursor simulation, synthesize inflow conditions using some sort of stochastic procedure. These procedures use random number generators to build a fluctuating velocity signal similar to those observed in turbulent flows. This is possible based on the assumption that a turbulent flow can be approximated from a set of low order statistics, such as mean velocity, turbulent kinetic energy, Reynolds stresses, two-point or two-time correlations. However, it is worth emphasizing that the resulting synthesized signals remain only a crude approximation of turbulence. From a statistical point of view, some crucial quantities, such as the dissipation rate, the turbulent transport or the pressure-strain term that appears in the Reynolds stresses balance are often not well reproduced. The dynamics of the turbulent eddies are not perfectly recovered, and the synthesized flow may undergo a transition to turbulence. Therefore, synthesized turbulence can have a structure that significantly differs from that of the real flow fields (Jarrin *et al.*, 2009).

2.2.1 White noise based synthetic turbulence generators

The most straightforward approach to build synthetic fluctuations is to generate a set of independent random numbers between zero and unity which can *mimic* the turbulence intensity at the inlet. Indeed, if the turbulent kinetic energy level k is known, it can be used to scale a random signal \mathcal{R}_{u_i} with zero mean and unity variance. Thus, the fluctuations exhibit the correct level of turbulent kinetic energy, which yields $u_i = \tilde{u}_i + \mathcal{R}_{u_i} \sqrt{2k/3}$, where \mathcal{R}_{u_i} is taken from independent random variables for each velocity component at each instant and location on the computational inlet plane. This procedure generates an isotropic random signal that reproduces both the mean velocity and turbulent kinetic energy levels. However, the signal generated does not present any two-point nor two-time correlations. The white noised based random fluctuations have their energy spectrum uniformly spread over all wave numbers and, as already stated above, this energy

will be quickly dissipated downstream of the inlet boundary. A more valuable approach for generating synthetic turbulence consists in creating bins of random data, which can then be processed using digital filters, so that the resulting set of processed data will display desired statistical properties, such as spatial and temporal correlations (Lund, 1998; Klein *et al.*, 2003).

2.2.2 Digital filters based synthetic turbulence generators

Klein *et al.* (2003) proposed a digital filtering procedure to remedy the lack of large-scale correlation in the inflow data generated from the above method. In one dimension the velocity signal $u'(j)$ at a point j is defined as a convolution or a digital linear non-recursive filtering, $u'(j) = \sum_{k=-N}^N b_k \mathcal{R}_{j+k}$, where \mathcal{R}_{j+k} is a series of random data generated at point $(j+k)$ with $\overline{\mathcal{R}_m} = 0$, $\overline{\mathcal{R}_m \mathcal{R}_m} = 1$ and b_k are the filter coefficients. The integer number N is related to the size of the filter support.

Following Klein *et al.* (2003), it is possible to generate a large amount of data, store and convect it through the inflow plane by applying Taylor's hypothesis. However, for the applications considered here, the inflow data will be generated on-the-fly.

It should be noted that the main parameters retained to evaluate this method are the choice of the length scales, which are directly connected to the filter support size, and the dimensions of the control volume. Thus, a given value of the characteristic length scale may be reproduced by correctly choosing the filter support size as well as the control volumes dimensions. However, as will be shown below, the length scales and, consequently, the filter support size strongly impact on the computational cost of the method. Finally, since a fixed computational grid is used here to assess the different turbulent inflow generators, the parameters retained to evaluate the method of Klein *et al.* (2003) will be the support size, only.

2.2.3 Synthetic turbulence generators based on Fourier techniques

To the authors best knowledge, Kraichnan (1970) was the first to use a Fourier decomposition to generate a synthetic fluctuating turbulent flow field. In Kraichnan's early work, the flow is initialized with a three-dimensional homogeneous and isotropic synthetic velocity field to study the diffusion of a passive scalar. Since velocity fluctuations are homogeneous in the three dimensions, they can be decomposed in the Fourier space, $\mathbf{u}'(\mathbf{x}) = \sum_{\mathbf{k}} \hat{\mathbf{u}}_{\mathbf{k}} e^{-i\mathbf{k}\cdot\mathbf{x}}$, where \mathbf{k} is a three-dimensional wave number vector. Each complex Fourier coefficient $\hat{\mathbf{u}}_{\mathbf{k}}$ defines an amplitude evaluated from a prescribed isotropic three-dimensional energy spectrum $E(|\mathbf{k}|)$ and a random phase $\theta_{\mathbf{k}}$, taken uniformly in the $[0, 2\pi]$ interval (Rogallo, 1981). The synthesized velocity field is thus given by $\mathbf{u}'(\mathbf{x}) = \sum_{\mathbf{k}} \sqrt{E(|\mathbf{k}|)} e^{-i(\mathbf{k}\cdot\mathbf{x} + \theta_{\mathbf{k}})}$. Several adaptations of Kraichnan's method were proposed throughout the years. Among them, important developments can be found in Lee *et al.* (1992) and Le *et al.* (1997). More recently, Smirnov *et al.* (2001) modified the method of Le *et al.* (1997) in such a manner that it becomes possible to obtain a turbulent velocity field by requiring statistical information only. The method of Smirnov *et al.* (2001) is capable of synthesizing non-homogeneous turbulence within a general framework. It relies on the Fourier decomposition, with Fourier coefficients computed from spectral data based on local turbulent time and length scales obtained at different

locations across the flow. This method, called *Random Flow Generation - RFG*, differs from the original proposal of Lee *et al.* (1992) since it does not use of Fourier transforms. It is based on scaling and coordinates transformation operations only, which, on non-uniform grids, are much more efficient. It is worth noting that this procedure requires specifying the characteristic integral length and time scales of turbulence, and the correlation tensor R_{ij} of the flow. These quantities can be obtained from experimental data, but some of them may also be approximated from preliminary RANS simulations.

2.2.4 Synthetic eddy method - SEM The synthetic eddy method (SEM), proposed by Jarrin *et al.* (2009), is based on the decomposition of the turbulent flow field into stochastic coherent structures. The corresponding eddy-structures are generated at the computational domain inlet plane and defined thanks to a shape-function $f_\sigma(x)$, which is intended to embrace turbulence spatial and temporal characteristics.

The synthetic eddy method can be introduced by using a one-dimensional scheme, in which the velocity component is generated within the range $[a, b]$. The shape-function of each turbulent spot features a compact support in $[-\sigma, \sigma]$, a position x_i , a length scale σ and is assigned a signal ε_i . In other words, the contribution $u^{(i)}(x)$ of a turbulent spot i to the velocity field, is defined as $u^{(i)}(x) = \varepsilon_i f_\sigma(x - x_i)$, with a location x_i randomly chosen within the range $[a - \sigma, b + \sigma]$ and where ε_i denotes a random step of value -1 or $+1$. The synthetic eddies are generated in an interval larger than $[a, b]$. This larger interval guarantees that the inlet points are surrounded by eddies. Finally, the resulting velocity field $u(x)$ at any location will be the sum of the contributions of all synthetic eddies located in the domain, $u(x) = \sum_{i=1}^N \varepsilon_i f_\sigma(x - x_i) / \sqrt{N}$, where N denotes the total number of synthetic eddies. The final velocity field u_i is then obtained from the above synthetic fluctuating velocity field u'_j , the velocity mean profile \bar{u}_i , and the Cholesky's decomposition a_{ij} of the Reynolds stress tensor: $u_i = \bar{u}_i + a_{ij}u'_j$.

3 Computational model

The mathematical and computational framework retained to proceed with the numerical simulation is now briefly presented. The interested reader may find a detailed presentation elsewhere (Vedovoto *et al.*, 2011). A hybrid approach in which the LES methodology is coupled with the transport of the scalar probability density function (PDF) is retained to describe the reactive cases. The method involves the numerical solution of partial differential equations (LES solver) together with stochastic differential equations (PDF solver). From the LES approach the Eulerian filtered variables are evaluated while stochastic differential equations (SDE) are solved using Lagrangian notional particles to simulate the modelled transport equation of the scalar PDF (Pope, 1985; Colucci *et al.*, 1998). The latter yields the one-point, one-time statistics of subgrid-scale scalar fluctuations and thus provides the LES solver with the corresponding filtered chemical reaction rate.

3.1 Set of filtered equations

The following simplifying assumptions are used: (a) fluid is considered as Newtonian, (b) body forces, heat

transport by radiation, Soret and Dufour effects are not addressed, (c) the model is developed for low Mach number flows, (d) we consider unity Lewis number values and equal molecular diffusion coefficients for all species, (e) heat losses are neglected. The mathematical model considers multi-species variable-density reactive flows, in which the primary transported variables are the density ρ , the three velocity components u_i , the specific enthalpy h and the mass fractions Y_k of the K chemical species ($k = 1, \dots, K$), the balance equations are:

$$\frac{\partial \bar{\rho}}{\partial t} + \frac{\partial \bar{\rho} \bar{u}_j}{\partial x_j} = 0, \quad (1)$$

$$\frac{\partial \bar{\rho} \bar{u}_i}{\partial t} + \frac{\partial \bar{\rho} \bar{u}_j \bar{u}_i}{\partial x_j} = \frac{\partial \bar{T}_{ij}}{\partial x_j} - \frac{\partial \tau_{ij}^{SGS}}{\partial x_j}, \quad (2)$$

$$\frac{\partial \bar{\rho} \bar{\phi}_\alpha}{\partial t} + \frac{\partial \bar{\rho} \bar{u}_j \bar{\phi}_\alpha}{\partial x_j} = \frac{\partial \bar{Q}_{\alpha,j}}{\partial x_j} - \frac{\partial \bar{Q}_{\alpha,j}^{SGS}}{\partial x_j} + \bar{S}_\alpha, \quad (3)$$

where the variable ϕ_α denotes the mass fraction of a chemical species or the enthalpy of the mixture, ($x_i, i = 1, 2, 3$) are the spatial coordinate, and t is the time. $T_{ij} = \tau_{ij} - p \delta_{ij}$ is the tensor of mechanical constraints including both a deviatoric (shear stresses τ_{ij}) and a spheric (pressure $p \delta_{ij}$) contribution, while $Q_{\alpha,j}$ denotes the component of the molecular diffusion flux of the scalar α in the direction j . In the above expression, $\tau_{ij}^{SGS} = (\bar{\rho} \bar{u}_i \bar{u}_j - \bar{\rho} \bar{u}_i \bar{u}_j)$ is the subgrid scale (SGS) stress tensor and $Q_{\alpha,j}^{SGS} = (\bar{\rho} \bar{u}_i \bar{\phi}_\alpha - \bar{\rho} \bar{u}_i \bar{\phi}_\alpha)$ represents the SGS scalar flux components, respectively. Finally, the last term in the RHS of Eq. (3), i.e. \bar{S}_α , denotes the filtered reaction rate. The above system is completed by an equation of state: $P = P_0(t) + p(\mathbf{x}, t)$, with $P_0(t)$ the thermodynamic pressure.

The unresolved momentum fluxes are expressed according to the Boussinesq assumption, $\tau_{ij}^{SGS} - \delta_{ij} \tau_{kk}^{SGS} / 3 = 2\mu_{SGS} (\tilde{S}_{ij} - \delta_{ij} \tilde{S}_{kk} / 3)$, where μ_{SGS} is the subgrid scale viscosity, and $\tilde{S}_{ij} = (\partial \tilde{u}_i / \partial x_j + \partial \tilde{u}_j / \partial x_i) / 2$ is the strain rate tensor of the resolved field (Ferziger & Peric, 1996). The eddy viscosity μ_{SGS} is obtained from the Smagorinsky closure, i.e., assuming that the small scales are in equilibrium, so that energy production and dissipation are in balance, which yields, $\mu_{SGS} = 2\bar{\rho} (C_s \Delta)^2 |\tilde{S}| = 2\bar{\rho} (C_s \Delta)^2 (2\tilde{S}_{ij} \tilde{S}_{ij})^{1/2}$, where C_s denotes the Smagorinsky constant. It is known that this closure can be excessively dissipative, especially near the walls, which is corrected herein by using a van Driest damping function (Ferziger & Peric, 1996). Finally, the SGS scalar flux is represented with a gradient law, $Q_{\alpha,j} = -\bar{\rho} \Gamma_{SGS} \partial \tilde{\phi}_\alpha / \partial x_j$, where $\tilde{\phi}_\alpha$ is the resolved scalar field and Γ_{SGS} denotes the subgrid diffusion coefficient evaluated from $\Gamma_{SGS} = 2\bar{\rho} (C_s \Delta)^2 |\tilde{S}| / Sc_{SGS}$ with Sc_{SGS} a subgrid scale turbulent Schmidt number.

3.2 Lagrangian Monte Carlo approach

The Lagrangian Monte Carlo approach offers the most classical framework to deal with the above PDF transport equation (Pope, 1985; Fox, 2003). In this approach, the joint scalar PDF is represented by an ensemble of notional particles (Fox, 2003), which evolve according to equivalent stochastic differential equations (SDE). A general framework to construct SDEs that are equivalent to the PDF transport equation is provided by Gardiner (2009).

In the present context, the SDEs that describe the trajectory of the particles in the physical space, \mathbf{x} , and in the sample space of the scalar field, Ψ , can be written as:

$$d\mathbf{x} = \left[\tilde{\mathbf{u}}(\mathbf{x}, t) + \frac{\partial \Gamma_{SGS}}{\partial x_i} \right] dt + \sqrt{2\Gamma_{SGS}} d\mathbf{W}(t), \quad (4)$$

$$d\Psi = [-\Omega_m(\Psi - \langle \Phi \rangle) + S(\Psi)/\rho(\Psi)] dt \quad (5)$$

where $\mathbf{W}(t)$ denotes the Wiener process, associated with a gaussian random variable featuring zero mean value and a variance dt (Fox, 2003), $\Omega_m = C_\omega(\Gamma + \Gamma_{SGS})/\Delta^2$ denotes the turbulent mixing frequency, with $C_\omega = 2.0$ the mechanical to scalar time scale ratio (Raman, 2004). The evolution of each notional particle occurs according to statistically independent increments $d\mathbf{W}(t)$, with a subgrid scale diffusion coefficient evaluated from the LES solver. The possible restrictions associated with the use of such an approach have been extensively discussed by Haworth (2010).

3.3 Numerical model

The essential features of the solver that has been used to conduct the numerical simulations are now presented and the reader may refer to Vedovoto *et al.* (2011) for further details.

The Lagrangian stochastic particles move through the physical space independently of each other. They are assigned spatial coordinates and represent mass. Due to the stochastic nature of motion, the number of particles present in a given elementary volume changes in time. In order to prevent particle accumulations in computational cells, and to keep small computational cells from running empty, particles are ascribed a relative weight and are periodically sampled (Zhang & Haworth, 2004). Following Pope (1985), the SDEs are discretized resorting to a fractional step method. In the next sections we proceed with the analysis of the different turbulent inflow generators by conducting the LES of the experimental test case of Moreau and coworkers. In a first step of the analysis, the corresponding wall bounded turbulent mixing layer flows is investigated in non reactive conditions and then attention is focused on the high-speed turbulent and reactive mixing layer.

4 Numerical simulations of a wall bounded turbulent mixing layer flow

The influence of the synthetic turbulence generators is studied via three-dimensional numerical simulations of a high speed mixing layer. The obtained results are compared with the experimental data provided by P. & A. (1977). The computational domain is a three-dimensional box with dimensions $(800 \times 100 \times 100)$ mm³, discretized with a finite volume mesh featuring $320 \times 100 \times 100$ cells in the x_1 , x_2 and x_3 directions, respectively. Since the numerical code developed has the capability of performing distributed computing, the computational domain is divided into 40 sub-domains. No-slip boundary conditions are imposed in the x_2 and x_3 directions. An advective boundary condition is used at the outflow. The Smagorinsky model is used with $C_s = 0.18$, and the Van-Driest damping function is applied at the walls. The Reynolds number, based on the initial width of the mixing layer, $\delta_m = 5$ mm, the mean velocity difference between the two inlet streams $U_r = 97.5$ m/s

and the value of the kinematic viscosity of air at 600 K is $Re = 3075$.

To perform the comparative analysis, the white noise synthetic turbulence generator is considered with fluctuation levels of 20% and 10% imposed on the streamwise and transverse velocity components respectively. For the simulations conducted with the method of Klein *et al.* (2003) the size of the filter support is set to 10, whereas 1,000 Fourier modes are retained for the simulations based on the method of Smirnov *et al.* (2001). For the simulation carried out using the method of Jarrin *et al.* (2009), 10k eddies are used.

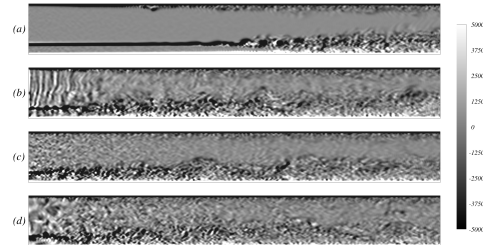


Figure 1. Component in x_2 -direction of the vorticity as obtained from the simulations carried out with the method: (a) white noise, (b) Klein *et al.* (2003), (c) RFG of Smirnov *et al.* (2001), and (d) SEM of Jarrin *et al.* (2009).

Figure (1), which depicts the vorticity component along direction x_2 , also provides a valuable insight into the behavior of the Smagorinsky model. It is commonly agreed that the Smagorinsky model is highly dissipative. This is one of the reasons that also explains why the white noise generator signal imposed at the inlet may be rapidly destroyed. However, provided that a more elaborated method is retained to generate the inflow turbulence, Fig. (1) confirms that a signal featuring large scales introduced in the domain is not so quickly dissipated, even when the Smagorinsky model is used.

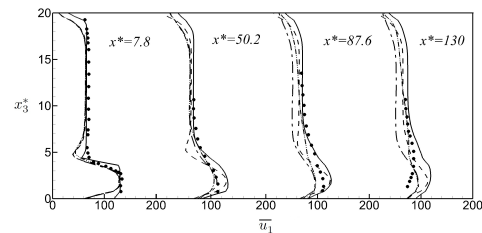


Figure 2. Mean longitudinal velocity profiles. (●): P. & A. (1977); RFG of Smirnov *et al.* (2001) (- - -); Klein *et al.* (2003) (- · - ·); white noise (- · · -); SEM of Jarrin *et al.* (2009) (—).

In order to assess quantitatively the methods implemented, Fig. (2) displays comparisons of the averaged u_1 -component of the velocity with experimental data at four distinct locations in the computational domain, for $x_2^* = 10$. The results confirm that the different methods provide an acceptable representation of the mean velocity field when compared with experimental data. However the need for an improved turbulent inflow generator becomes clear to reproduce the levels of velocity fluctuations. Indeed, it can be seen in Fig. (3) that the superimposition of white noise on the mean velocity is unable to recover the experimental data in the first half of the computational domain along the

August 28 - 30, 2013 Poitiers, France

x_1 -direction. In contrast, the results obtained with the methods of Klein *et al.* (2003), Smirnov *et al.* (2001), and Jarrin *et al.* (2009) display a more satisfactory level of agreement with experimental data at the same location.

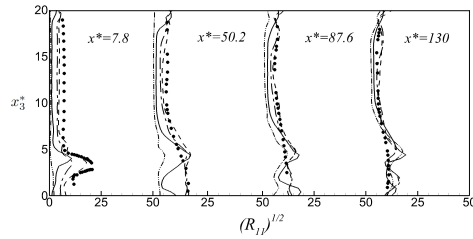


Figure 3. $\sqrt{R_{11}}$ stress tensor component. (●): P. & A. (1977); RFG of Smirnov *et al.* (2001) (- -); Klein *et al.* (2003) (- · -); white noise (- · · -); SEM of Jarrin *et al.* (2009) (—).

From the computational cost point of view, it is clear that the better quality of the results obtained with the methods of Klein *et al.* (2003), Smirnov *et al.* (2001) and Jarrin *et al.* (2009) require longer CPU times than that associated with the simple superimposition of a white noise on the mean inlet velocity. However, for the present test case, the simulations conducted with the methods of Klein *et al.* (2003) and Smirnov *et al.* (2001) correspond to approximately the same computational cost, i.e., about 40% more than that associated with the white noise methodology, for the former, and 35% for the latter. The cost associated with the numerical simulations conducted with the SEM is 55% higher than that conducted with the white noise. The methods of Klein *et al.* (2003) and Smirnov *et al.* (2001), therefore, appear as particularly attractive. Nevertheless, there are two crucial differences between the methods of Klein *et al.* (2003) and Smirnov *et al.* (2001). The first does not yield temporal correlations, only spatial correlations are guaranteed. Moreover, the method of Smirnov *et al.* (2001) generates a divergence-free velocity field at the inlet.

5 Reactive flows simulations

Although there is already some literature available to describe the influence of realistic turbulent inflow data prescription on non-reactive flows (Tabor & Baba-Ahmadi, 2010), such an analysis of the turbulent inflow data effects is much less common for turbulent reactive flows. In this last subsection, a set of two-dimensional reactive flow simulations is conducted to evidence such effects. The computational domain is a three-dimensional box with dimensions $(800 \times 2 \times 100)$ mm³. It is discretized with a mesh of $320 \times 1 \times 100$ control volumes in the x_1 , x_2 and x_3 -direction, respectively. Periodicity and no-slip boundary conditions are imposed along x_2 the x_3 -directions respectively. The computational domain is divided into 8 parallel regions. The other parameters remain the same as those retained for non reactive cases. Concerning the turbulent inlet generators, for the reactive flow simulations we retain the set-up of the non-reactive simulations.

To proceed with the mathematical modelling of the chemical source term, we retain a single step, global, and irreversible reaction that involves the progress variable, i.e., a normalized temperature defined by $c \equiv (T - T_u)/(T_b - T_u)$ where the subscripts u and b denote fresh reactants and fully burned gases conditions respectively.

The initial and boundary condition for the mean value of the progress variable at $x_1^* = 0$, are set with a hyperbolic profile, separating the streams of gases from the auxiliary burner ($c_q = 1$; $T_b = 2000$ K) and of the main duct ($c_p = 0$; $T_u = 560$ K). Concerning the Monte Carlo simulation, 50 particles per control volume are used and the Milstein scheme is employed for the numerical integration of the system of SDEs.

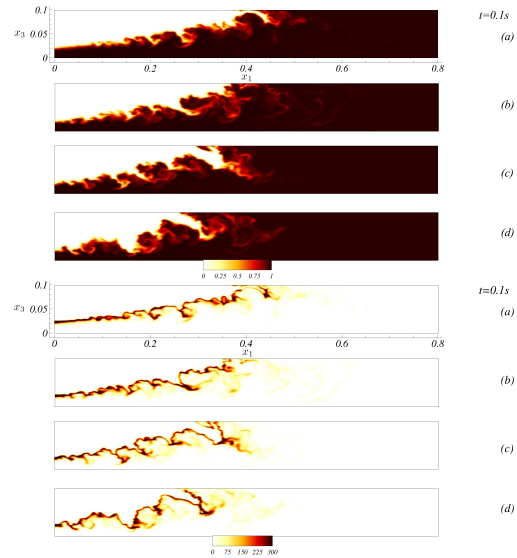


Figure 4. Instantaneous fields of chemical reaction progress variable c - top, and chemical reaction rate $S(c)$ - bottom. The subfigures (a), (b), (c), and (d) display results of simulations with the respective inlet boundary condition methods: white noise; Klein *et al.* (2003), RFG of Smirnov *et al.* (2001) and SEM of Jarrin *et al.* (2009)

Figure (4) shows instantaneous fields of the chemical reaction progress variable c and the filtered chemical reaction rate $S(c)$ for the present set of numerical simulations. The method of turbulent inflow data generation clearly influences the shear layer spreading rate as well as the position of the instantaneous filtered flame front. For instance, if we consider the subfigure (a) of Fig. (4), the longitudinal span of the turbulent flame front obtained with the white noise is larger than the one obtained using the other three methods.

Concerning the influence of the inlet boundary condition, we observe in Fig. (5) that accounting for a fluctuation spectrum always gives rise to a shorter and thicker flame brush. The length of the 2D flame brush, based on the location of the iso-line $\langle c \rangle = 0.9$ in the x_1 direction, is found to be 560 mm for the simulation carried out with the superimposition of a white noise, while for the methods of Klein *et al.* (2003), Smirnov *et al.* (2001) and Jarrin *et al.* (2009) the lengths are 543, 497 and 414 mm respectively.

6 Conclusion

Large Eddy Simulations of both reactive and non reactive turbulent channel flows of methane/air mixtures have been conducted with special emphasis placed on the influence of turbulent inlet Boundary Conditions. The analysis undoubtedly confirms the sensitivity of the obtained results to the choice of the synthetic turbulence generator retained at the inlet of the computational domain. The computational results of the corresponding LES are investigated in details

August 28 - 30, 2013 Poitiers, France

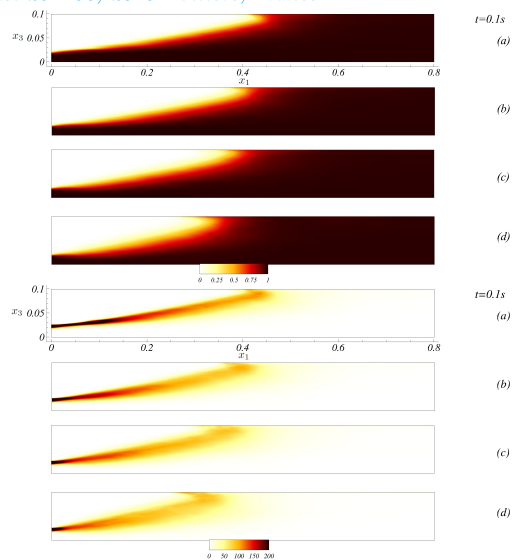


Figure 5. Averaged fields of chemical reaction progress variable c - top, and chemical reaction rate $S(c)$ - bottom. The subfigures (a), (b), (c), and (d) are results of simulations with the respective inlet boundary condition methods: white noise ; Klein *et al.* (2003), RFG of Smirnov *et al.* (2001) and SEM of Jarrin *et al.* (2009)

and the quality of the agreement with experimental data is found to be significantly improved by resorting to elaborated synthetic turbulence generators that account for the large scale dynamics and coherence. The results obtained for reactive flow conditions also clearly emphasize the influence of the retained model on the chemical rate statistics, which confirms the importance of this issue for the LES of turbulent reactive flows. From the computational cost point of view, the methods of Klein *et al.* (2003), Smirnov *et al.* (2001) and Jarrin *et al.* (2009) require longer CPU time than the method associated with the simple superimposition of a white noise on the mean velocity inlet profile. For the present applications, the additional CPU costs lie between 35% for the method of Smirnov *et al.* (2001), and 55% for the method of Klein *et al.* (2003), which remains moderate considering the potential improvements that may be obtained from their use.

7 Acknowledgements

The authors would like to thanks *Capes*, *FAPEMIG*, *CNPq* and *Petrobras* for financial support. This work was performed while the third author was on leave from CNRS.

REFERENCES

Bodony, D 2006 Analysis of sponge zones for computational fluid mechanics. *Journal of Computational Physics* **212** (2), 681–702.

Colucci, P. J., Jaber, F. a., Givi, P. & Pope, S. B. 1998 Filtered density function for large eddy simulation of turbulent reacting flows. *Physics of Fluids* **10** (2), 499.

Druault, P., Lardeau, S., Bonnet, J. P., Coiffet, F., Delville, J., Lamballais, E., Largeau, J. F. & Perret, L. 2004 Generation of three-dimensional turbulent inlet conditions for large-eddy simulation. *AIAA Journal* **42**, 447–456.

Ferziger, J.H. & Peric, M. 1996 *Computational methods for fluid dynamics*. Springer.

Fox, R. O. 2003 *Computational models for turbulent reacting flows*. Cambridge University Press.

Gardiner, C 2009 *Stochastic methods: a handbook for the natural and social sciences*. Springer.

Haworth, D.C. 2010 Progress in probability density function methods for turbulent reacting flows. *Progress in Energy and Combustion Science* **36** (2), 168–259.

Jarrin, N., Prosser, R., Uribe, J.-C., Benhamadouche, S. & Laurence, D. 2009 Reconstruction of turbulent fluctuations for hybrid RANS/LES simulations using a Synthetic-Eddy Method. *International Journal of Heat and Fluid Flow* **30** (3), 435–442.

Klein, M., Sadiki, A. & Janicka, J. 2003 A digital filter based generation of inflow data for spatially developing direct numerical or large eddy simulations. *Journal of Computational Physics* **186**, 652–665.

Kraichnan, R H 1970 Diffusion by a random velocity field. *Physics of Fluids* **13** (1), 22–31.

Le, H, Moin, P & Kim, J 1997 Direct numerical simulation of turbulent flow over a backward-facing step. *Journal of Fluid Mechanics* **330**, 349–374.

Lee, S., Lele, S. K. & Moin, P. 1992 Simulation of spatially evolving turbulence and the applicability of Taylor's hypothesis in compressible flow. *Physics Of Fluids A Fluid Dynamics* **4** (May 1991), 1521–1530.

Lumley, J. L. 1967 The structure of inhomogeneous turbulence. In *Atmospheric turbulence and wave propagation* (ed. A. M. Yaglom & V. I. Tatarski), pp. 166–178. Moscow: Nauka.

Lund, T 1998 Generation of turbulent inflow data for spatially-developing boundary layer simulations. *Journal of Computational Physics* **140** (2), 233–258.

Magre, P., Moreau, P., Collin, G., Borghi, R. & Péralat, M. 1988 Further studies by cars of premixed turbulent combustion in a high velocity flow. *Combustion and Flame* **71** (2), 147 – 168.

Orlanski, I 1976 A simple boundary condition for unbounded hyperbolic flows. *Journal of Computational Physics* **21** (3), 251 – 269.

P., Moreau & A., Boutier 1977 Laser velocimeter measurements in a turbulent flame. *Symposium (International) on Combustion* **16** (1), 1747 – 1756.

Pope, S B 1985 Pdf methods for turbulent reactive flows. *Progress in Energy and Combustion Science* **11** (2), 119–192.

Raman, V 2004 Hybrid finite-volume/transported PDF simulations of a partially premixed methane-air flame. *Combustion and Flame* **136** (3), 327–350.

Rogallo, R S 1981 Numerical experiments in homogeneous turbulence. *Nasa Technical Memorandum* **81** (81835).

Smirnov, A., Shi, S. & Celik, I. 2001 Random flow generation technique for large eddy simulations and particle-dynamics modeling. *Journal of Fluids Engineering* **123**, 359–371.

Tabor, G.R. & Baba-Ahmadi, M.H. 2010 Inlet conditions for large eddy simulation: A review. *Computers & Fluids* **39** (4), 553–567.

Vedovoto, J. M., da Silveira Neto, A., Mura, A. & Figueira da Silva, L. F. 2011 Application of the method of manufactured solutions to the verification of a pressure-based finite-volume numerical scheme. *Computers & Fluids* **51** (1), 85 – 99.

Zhang, Y Z & Haworth, D C 2004 A general mass consistency algorithm for hybrid particle/finite-volume pdf methods. *Journal of Computational Physics* **194** (1), 156 – 193.